

Theory of excess-electron states in classical rare-gas fluids

D.-Y. Kuan and C. Ebner

Department of Physics, The Ohio State University, Columbus, Ohio 43210

(Received 22 July 1980)

Localized excess-electron states are investigated using the density-functional formalism previously developed by Ebner, Saam, and Stroud for nonuniform classical fluids. The electron-atom interactions used contain a short-range effective core repulsion and a long-range polarization attraction. The interatomic interaction is a 6-12 potential. Some results are in agreement with previous density-functional calculations by Ebner and Punyanitya, who use a contact potential for the electron-atom interaction, in that no localized states are found in dilute helium and neon gases, while localized states are found in dense helium gas and liquid neon close to the liquid-gas coexistence curve. However, our present calculations disagree with the earlier ones in that they predict the localized states in liquid neon to be stable even at pressures much larger than the saturated vapor pressure, a consequence, we believe, of our inclusion of the polarization potential in the electron-atom interaction. We also find that localized states in the form of short-lived droplets are possible in argon and xenon gases close to the critical point. This finding is consistent with recent observations by Freeman and Huang of electron mobilities in these gases.

I. INTRODUCTION

During the past few years much work has been done with the goal of understanding the physics of excess-electron states in nonpolar fluids, especially in rare-gas fluids.¹ The investigations have focused on the elucidation of observed small electron mobilities on the order of 10^{-2} to 10^{-3} cm²/V sec in liquid helium,²⁻⁵ dense gaseous helium,⁶⁻¹⁰ and liquid neon.^{11,12} Recently it also has been found that in both gaseous xenon and gaseous argon near the critical point there are sharp decreases in the electron mobility.^{13,14} These low-mobility electron states are classified as localized state in contrast to quasifree or extended electron states which are characterized by large mobilities on the order of 10^1 to 10^4 cm²/V sec. Numerous theoretical descriptions have been given of localized or reduced mobility electron states in the rare-gas fluids.^{7,15-18} The most generally used description for these states in helium and neon is the "bubble" model, according to which the electron creates a cavity or bubble around itself in the fluid and then becomes trapped within this bubble. Earlier calculations using this model predict that excess-electron states should be localized in liquid helium and in liquid neon^{19,20} but quasifree in liquid argon.¹⁹ These results seem to be consistent qualitatively with experimental observations.^{2-12,21-23}

As for the localization of electrons in xenon and argon near the critical point, it is believed to be small fluctuations in the local density of the fluid which serve as trapping centers for the electrons.^{13,14,18} A "droplet" model has been suggested to describe these localized electron states in highly polarizable gases and it has

been predicted that the localization of electrons in xenon is possible.²⁴

From thermodynamics the condition that electron bubble (or droplet) states be stable relative to quasifree electron states is that the free energy of the former be lower than that of the latter. A relatively simple and qualitatively correct theory for calculating the quasifree electron states in monatomic fluids has been given by Springett *et al.*^{19,25} The Wigner-Seitz method²⁶ which assumes that each fluid particle occupies a sphere of volume equal to the inverse particle density was used. Also, the interaction between the electron and a fluid atom was chosen to include the long-range attractive polarization potential and a short-range repulsive potential. The effective potential acting on the electron inside the Wigner-Seitz sphere is then the sum of the bare potential from the atom at the center of the sphere and the mean potential produced by the other atoms of the fluid.

A variety of procedures have been previously adopted to estimate the free energy of the fluid with a bubble state in it. Some of these theories have assumed that there is an abrupt boundary between the bubble and the fluid with the fluid density equal to zero inside and equal to the density of uniform fluid outside.^{19,20} The insertion of the electron into the fluid and the formation of a bubble state will produce a free-energy change which includes the ground-state energy of the localized electron, the surface and volume free energy of the bubble and the polarization energy of the medium surrounding the bubble. Hence, the condition for a stable-electron bubble state is that this free-energy change is less than the free-energy change accompanying the insertion of an electron into a quasifree state.

Such a description of the bubble state may be regarded as a very simple density-functional theory. A further step along this line of investigation was taken by Hernandez²⁷ who formulated the free energy of a nonuniform ideal gas as a functional of its density and then determined the equilibrium configuration in the presence of an electron by minimizing this functional. The principal approximations in this work are the treatment of the fluid as an ideal gas and the use of a contact potential to describe the electron-atom interaction.

Recently, Ebner and Punyanitya²⁸ (referred to hereafter as EP) have applied the density-functional formalism of Ebner, Saam, and Stroud²⁹ to the problem of localized excess-electron states in rare-gas fluids. The correlations in the fluid are built into this formalism as is the liquid-gas phase transition. Among other things, the formalism is capable of predicting nonmonotonic behavior of the particle-density profile. The intermolecular potential is taken to be the Lennard-Jones (6-12) potential and correlations are treated within the Percus-Yevick approximation. In EP a simple contact potential is used to represent the electron-atom interaction. This choice simplifies the computations enormously but fails to adequately represent the long-range attractive polarization potential acting between an atom and the electron.

The results of EP agree with previous theories in that localized bubble states are found in sufficiently dense helium gas and in liquid neon close to the liquid-gas coexistence curve. They also predict that the localized bubble states in neon become unstable at sufficiently large liquid densities. This contradicts the previous findings using the ideal-gas model²⁷ that electron bubble states are stable even at high liquid densities in neon. In the search for dropletlike localized states, they find no such states in any rare gases and thus fail to give any support to the recent claim by Huang and Freeman^{13, 14} that the observed decrease in the excess-electron mobility in both xenon and argon vapor near the critical point is a consequence of such droplets. However, if the scattering length in the contact potential is given a plausible density dependence as suggested in Ref. 14, then droplet states result.

The purpose of the present study is to improve the calculations reported in EP by changing the electron-atom interaction from a simple contact potential to a physically more reasonable one which includes a short-range repulsion and a long-range polarization attraction. The remainder of the paper is organized as follows. Section

IIA provides a very brief review of the density-functional formalism as applied to the excess-electron problem and II B, a description of the procedure used to arrive at reasonable electron-atom potentials. Section III presents the results of the computations, Sec. III A pertaining to the determination of the electron-atom potentials and Sec. III B, to the density-functional calculations of the localized states in the various rare-gas fluids. Section IV contains a summary.

II. FORMALISM

A. Density functional

The density functional used here is identical to that in EP which is, in the absence of the electron, the same as that introduced in Ref. 29. The difference between the free energies of the localized state and the lowest extended state is $\Delta\Omega$ where $\Delta\Omega$ is found by minimizing the following functional with respect to variations of $n(\vec{r})$ at fixed temperature T and chemical potential μ :

$$\begin{aligned} \Delta\Omega[n] = & \Delta E_e[n] + \int d^3r [f(n(\vec{r})) - \mu n(\vec{r}) + P_0] \\ & + \frac{kT}{4} \int d^3r d^3r' C(|\vec{r} - \vec{r}'|; \bar{n}) \\ & \times [n(\vec{r}) - n(\vec{r}')]^2, \end{aligned} \quad (1)$$

where $\Delta E_e[n]$ is the lowest energy eigenvalue of the one-electron Schrödinger equation

$$\begin{aligned} -\frac{\hbar^2}{2m_e} \nabla^2 \psi_e(\vec{r}) + \int d^3r' v(|\vec{r} - \vec{r}'|) [n(\vec{r}') - n_0] \psi_e(\vec{r}) \\ = \Delta E_e[n] \psi_e(\vec{r}). \end{aligned} \quad (2)$$

In these equations, $n(\vec{r})$ is the atomic number density in the fluid; $v(r)$, the electron-atom interaction; $f(n)$, the Helmholtz free-energy density of the uniform fluid at n and T ; and $C(r; \bar{n})$, the direct correlation function in the uniform fluid at \bar{n} and T . The pressure P_0 is that of a uniform fluid at μ and T while n_0 is the number density of this fluid. We determine f and C and choose \bar{n} in the manner described in Ref. 29. The interaction between fluid atoms is taken to be the Lennard-Jones (6-12) potential.

$$V(r) = 4\epsilon \left[\left(\frac{\sigma}{r} \right)^{12} - \left(\frac{\sigma}{r} \right)^6 \right]. \quad (3)$$

The parameters ϵ and σ used for the various rare gases, taken from Hirschfelder *et al.*³⁰ are listed in Table I. The relationship between this functional and an exact one³¹ as well as the reliability of the functional in a specific one-dimensional application are examined in a recent publication.³²

Within the context of this formalism, if a minimum of $\Delta\Omega[n] \equiv \Delta\Omega_{\min}$ can be found for a local-

TABLE I. Parameters entering the interatomic and electron-atom potentials for the various rare gases.

| Element | $\sigma(\text{\AA})$ | $\epsilon/k(K)$ | $\alpha(a_0^{-3})$ | $\sigma_e(a_0)$ | N |
|---------|----------------------|-----------------|--------------------|-----------------|-----|
| He | 2.556 | 10.2 | 1.36 | 1.75 | 10 |
| Ne | 2.789 | 35.7 | 2.65 | 1.48 | 10 |
| Ar | 3.405 | 119.76 | 11.0 | 2.07 | 10 |
| Kr | 3.600 | 171.0 | 16.6 | 2.30 | 10 |
| Xe | 4.100 | 221.0 | 27.0 | 2.45 | 10 |

ized electron state with some $n_e(\vec{r}) \neq n_0$, then this state is stable if $\Delta\Omega_{\min} < 0$ and metastable if $\Delta\Omega_{\min} > 0$; $n_e(\vec{r})$ is the fluid particle density in this state. If no such minimum exists, then localized states are unstable. Further, that extended state which has the lowest free energy has a constant density n_0 and an electronic wave function which is also a constant. The potential which the fluid exerts upon the electron is computed as a mean field and so the formalism is inappropriate if the electron-atom interaction is not integrable. In order to accommodate this fact we have chosen this interaction in the manner described immediately below.

B. Electron-atom potential

We consider first a bare interaction consisting of the attractive polarization potential and a parametrized repulsive core,

$$v'(r) = \frac{e^2}{2a_0} \left[\left(\frac{\sigma_e}{r} \right)^N - \frac{\alpha a_0}{r^4} \right]; \quad (4)$$

α is the atomic polarizability and a_0 and e are the Bohr radius and electronic charge. We have used the polarizabilities given by O'Malley³³; these are listed in Table I. The parameters σ_e and N are determined by fitting the very low-energy s -wave phase shifts δ_0 for electron-atom scattering to experimental or theoretical determinations of these phase shifts for the various rare gases.³⁴⁻³⁷ Our procedure for calculating the phase shifts is straightforward, being based on the standard formulation³⁸ of phase shifts in terms of solutions to the radial Schrödinger equation, the latter being obtained numerically using an algorithm suggested by Fox and Goodwin.³⁹

The rationale for introducing the repulsive core into $v'(r)$ is that the wave function of the scattered or unbound electron must be orthogonal to the atomic orbitals and so must have a large kinetic energy in the region of the atomic core. In the spirit of pseudopotential theory, we have represented the exchange repulsion effect with the r^{-N} part of $v'(r)$. We must also normalize the phase shifts in such a way that $\delta_0 \rightarrow 0$ as the

incident electron energy goes to zero.

Those sets of parameters N and σ_e which yield a good fit to the low-energy s -wave phase shifts do not in general reproduce well the p -wave phase shifts. The reason for this is that the exchange repulsion arises from the orthogonality requirement on the unbound electron wave function; this requirement varies with the different angular momentum states and so the repulsion will be angular momentum dependent. The most extreme case arises for helium atoms which do not exert any exchange repulsion on an incident electron with nonzero relative angular momentum. We do not concern ourselves with the $l=1$ and higher partial waves because in the applications considered here electrons have sufficiently low energy that when they are within an atomic radius of any given atom, they are predominantly in an $l=0$ state relative to that atom.

Equation (4) represents a bare electron-atom potential suitable for describing the interaction between an electron and a single atom. In calculations of fluid properties one must include the screening of the polarization interaction. Assuming local screening, we write the screened interaction as

$$v'_{sc}(r) = \frac{e^2}{2a_0} \left[\left(\frac{\sigma_e}{r} \right)^N - \frac{\alpha a_0}{r^4} f(r) \right]. \quad (5)$$

Our choice of the screening function $f(r)$ is the same as that employed in Ref. 19,

$$f(r) = \begin{cases} 1, & r < r_s \\ (1 + \frac{8}{3} \pi n_0 \alpha)^{-1}, & r > r_s, \end{cases} \quad (6)$$

where $r_s = (3n_0/4\pi)^{1/3}$. In the process of making this choice we performed Wigner-Seitz calculations of the lowest energy extended electron states in the rare-gas fluids, comparing the resulting energies with the ionization potentials E_0 measured by Sommer⁴⁰ and by Tauchert *et al.*⁴¹ For Ar and Ne, we used not only the screening function of Eq. (6) but also no screening, $f=1$, and full screening, $f=(1 + \frac{8}{3} \pi n_0 \alpha)^{-1}$ for all r . All things considered, Eq. (6) seemed the best simple compromise.

As for the Wigner-Seitz calculations, we followed the prescription of Springett *et al.*¹⁹ but avoided some of their approximations. In a fluid of density n_0 , we construct a spherical cell of radius r_s around an atom located at $\vec{r}=0$. The one-electron potential at a point \vec{r} in this cell, $V_1(r)$, is taken as the sum of the potential produced by the atom at the origin, $v'(r)$, plus the mean potential produced by atoms outside of the cell distributed with a density $n_0 g(\vec{r}')$ at position \vec{r}' ; g is the pair distribution function of the fluid

and was obtained by solving the Percus-Yevick equation. Thus

$$V_1(r) = v'(r) + n_0 \int_{r', r_s} d^3r' v'_{sc}(|\vec{r} - \vec{r}'|) g(r'). \quad (7)$$

We then solved the appropriate Schrödinger equation in the cell,

$$-\frac{\hbar^2}{2m} \nabla^2 \psi(r) + V_1(r) \psi(r) = E_{ws} \psi(r), \quad (8)$$

subject to the boundary condition $d\psi/dr|_{r_s} = 0$, to obtain the lowest energy eigenvalue E_{ws} for comparison with the measured ionization potential in each of the rare-gas fluids.

The final adjustment that we must make in the electron-atom potential in order that it be appropriate for use in the density functional is to make it integrable. In any event, an infinite hard core is not a reasonable representation of the exchange repulsion. We use it up to this point principally for convenience. The change we now make is to replace $v'_{sc}(r)$ at distances less than the cutoff radius r_c by its value of r_c ; that is, we use an electron-atom potential in the form

$$v(r) = \begin{cases} v'_{sc}(r_c), & r < r_c \\ v'_{sc}(r), & r > r_c \end{cases} \quad (9)$$

in all density-functional applications. The cutoff radius r_c is determined by the criterion that the energy of the lowest energy extended state in the mean-field approximation should be the same as that computed in the Wigner-Seitz model,

$$E_{ws} = n_0 \int d^3r v(r). \quad (10)$$

III. RESULTS OF THE COMPUTATIONS

A. Electron-atom potentials

The electron-atom potential as given by Eq. (4) has been fit to calculations of δ_0 for neon and argon,³⁵ to measurements of δ_0 for krypton³⁶ and for helium,³⁴ and to the scattering length inferred from the cross-section measurements of Ramsauer and Kollath for xenon.³⁷ The range of electron energies that are important in the systems we consider is easily estimated. An electron localized in a region of space of size D has a kinetic energy on the order of $\epsilon_0 \cong \hbar^2 \pi^2 / 2m D^2$ and a wave number $k_0 \cong \pi/D$. The typical bubble size is $10 a_0$ to $20 a_0$ so that $k_0 \lesssim 0.3 a_0^{-1}$ and $\epsilon_0 \lesssim 2$ eV. Hence we were careful to get the best fit in this small wave-number regime. The first and most careful fits, in which both N and σ_e were varied extensively, were done for Ne and Ar using Thompson's calculated phase shifts at $k < 2 a_0^{-1}$. We found that the quality of the fit

does not depend a great deal on N for $8 \lesssim N \lesssim 12$. Consequently, we have simply taken $N=10$ and then chosen σ_e to obtain the best fit of δ_0 to Thompson's calculations in the appropriate wave-number regime. The results for Ar with $\sigma_e = 2.07 a_0$ are shown in Fig. 1; at small k , our s -wave phase shift is virtually indistinguishable from Thompson's. The p -wave phase shift δ_1 is also shown. As expected from the discussion in Sec. II B the fit is not good, but that is of no consequence in our applications.

For Ne, Ar, and He, N was also set equal to 10 and similar fits to δ_0 were performed; for Xe, N was set equal to 10 and σ_e was fit to the measured scattering length. The resulting values of σ_e are listed in Table I.

The next step is to introduce local screening into the polarization interaction in the manner expressed by Eq. (5) and then to do Wigner-Seitz calculations of the lowest energy quasifree excess-electron states using Eqs. (7) and (8) at

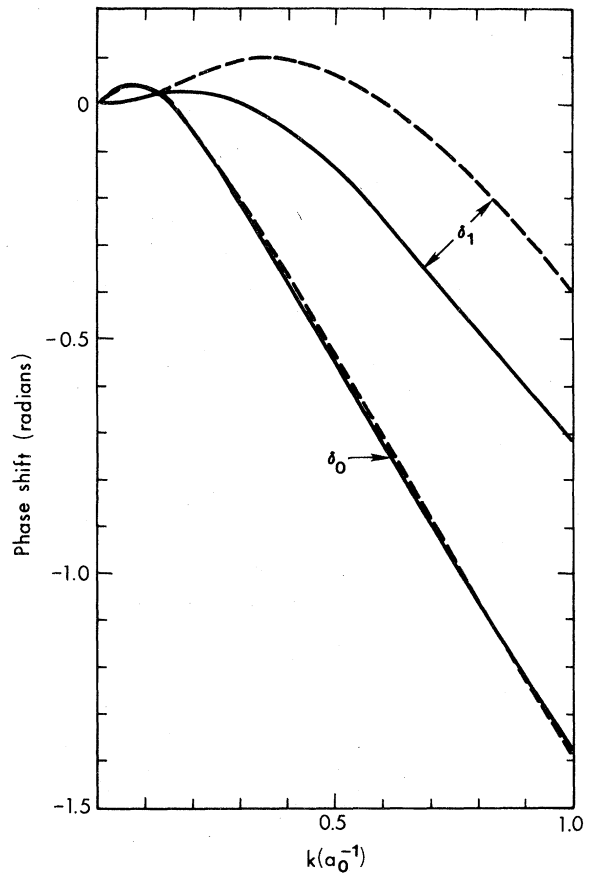


FIG. 1. The s -wave and p -wave phase shifts for the scattering of an electron from an argon atom as functions of the incident electron wave number. The solid lines (—) are from Ref. 35 while the dashed lines (---) are the result of our fit for $\sigma_e = 2.07 a_0$ and $N=10$.

densities and temperatures close to those at which the ionization potentials have been measured.^{40, 41} In all cases, the screening function of Eq. (6) was employed; for Ne and Ar, E_{ws} was also found using no screening and full screening. The results are shown, along with the measured ionization potential, in Table II; densities and temperatures are expressed in dimensionless form with $n_0^* = n_0 \sigma^3$ and $T^* \equiv kT/\epsilon$ where σ and ϵ are the range and depth parameters of the interatomic Lennard-Jones potential of the appropriate rare-gas element. Comparison of the various calculated and experimental energies shows, first, that screening has an increasingly large effect on E_{ws} as the atomic number of the atoms increases, reflecting the growing importance of the polarization potential and, second, that the use of Eq. (6) to describe the screening seems quite reasonable.

The final adjustment to the potential needed for use in the density functional is the replacement of the hard core by something integrable. We introduce a cutoff radius r_c and set the electron-atom potential equal to a constant for all $r < r_c$ as described by Eq. (9). The cutoff radii are determined from the criterion expressed in Eq. (10) using the energies from the Wigner-Seitz calculations. The potential $v(r)$ in the core region is sufficiently large—on the order of some tens of electron volts—that had the cutoff potential been used in place of Eq. (4) to determine the parameter σ_e from scattering phase shifts at low energy, there would be very little difference in the outcome.

B. Density-functional calculations

We now turn to consideration of the results for the free energies and density profiles of localized

states obtained from the density-functional formalism. The relative functional $\Delta\Omega[n]$ given by Eqs. (1) and (2) is minimized using a parametrized trial function for $n(\vec{r})$. Choosing $\vec{r} = 0$ as the center of the localized state and assuming rotational invariance, we have employed

$$n(r) = n_0 [1 - \delta / (e^{(r-\beta)/\gamma} + 1)]; \quad (11)$$

δ is positive or negative depending on whether the nonuniformity is more nearly a bubble or a droplet, β is essentially the radius of the nonuniform region, and γ is a measure of the width of its surface. The parameters β , γ , and δ are varied on a grid of adjustable size until minima of $\Delta\Omega[n]$ are obtained. For any given μ and T , minimization is performed for several sets of initial parameters to ensure that the minima are reproducible. The trial function of Eq. (11) can become negative at small r if δ is sufficiently large. For all r such that this occurs we set $n(r)$ equal to zero.

A trial function which includes more parameters to allow for possible oscillatory behavior of $n(\vec{r})$ near the bubble-liquid interface has been used in EP. Oscillatory profiles have actually been predicted for a fluid pressed against a hard wall²⁹ or for a fluid in contact with a wall that exerts a long-range van der Waals force on its atoms.⁴² The conclusions of EP, however, are that only monotonic density profiles appear in the bubble states, even at high liquid density.

One might *a priori* feel that it is important to use a trial function more flexible than that in Eq. (11) to allow for possible oscillations in the density. We may argue, on the basis of similar calculations for a model one-dimensional system,³² that oscillations are only likely when the interface is narrow and the fluid density change

TABLE II. Comparison of the measured ionization energies of an excess electron in the rare-gas fluids and the energy calculated in the Wigner-Seitz model.

| T^* | Experiment | | Element | T^* | Theory | |
|-------|------------|--------------------|---------|-------|---------|--------------------|
| | n_0^* | V_0 (eV) | | | n_0^* | E_{ws} (eV) |
| 0.41 | 0.36 | 1.05 ± 0.05^a | He | | | |
| 0.70 | 0.805 | 0.67 ± 0.05^b | Ne | 0.70 | 0.80 | 0.60 |
| | | | | 0.70 | 0.80 | 0.57 ^c |
| | | | | 0.70 | 0.80 | 0.65 ^d |
| 0.73 | 0.846 | -0.20 ± 0.02^b | Ar | 0.70 | 0.85 | -0.30 |
| | | | | 0.70 | 0.85 | -0.44 ^c |
| | | | | 0.70 | 0.85 | -0.09 ^d |
| 0.72 | 0.826 | -0.42 ± 0.05^b | Kr | 0.70 | 0.80 | -0.58 |
| 0.75 | 0.936 | -0.64 ± 0.05^b | Xe | 0.70 | 0.90 | -1.10 |

^a From Ref. 40.

^b From Ref. 41.

^c With no screening.

^d With full screening.

is large. This is the case only for bubble states in fluids at high pressure and density. In those materials for which bubble states are stable anywhere (helium and neon) we find that they are stable at high densities for monotonic profiles. Even if nonmonotonic profile should lower the bubble free energy further, that would not affect the qualitative conclusion that the bubble is stable. Hence we did not feel that the added complexity and consumption of computer time necessitated by a nonmonotonic trial function was desirable.

We now consider in turn our results for He, for Ne, and for Ar, Kr, and Xe. In each case comparison is made with the calculations of EP. For helium gas, it is found in EP that the electron bubble state is relatively less stable in the density-functional description than in the ideal-gas model using the same electron-atom interaction. The present calculations, based on an improved electron-atom interaction, predict increased stability of the bubble states. In Fig. 2 we plot the free energy difference $\Delta\Omega$ in units of ϵ against n_0^* at $T^*=7.7$. The curve IG results from the ideal-gas model while DF1 and DF2 are the predictions of the previous and present

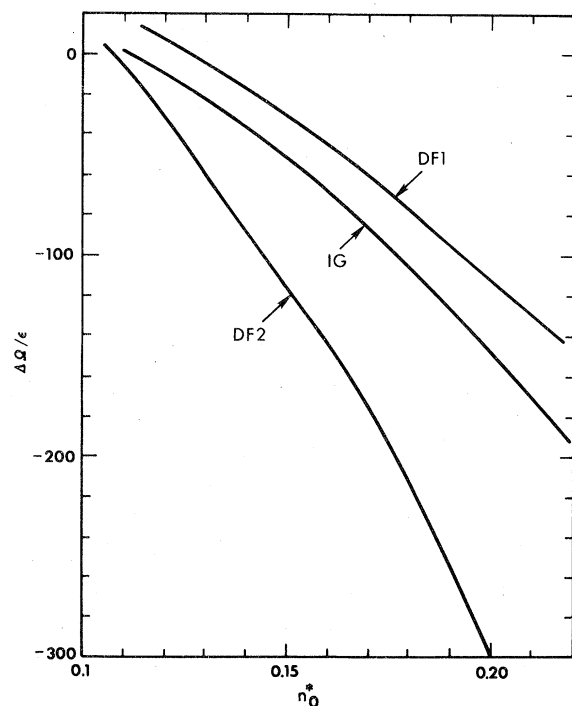


FIG. 2. Reduced free-energy differences $\Delta\Omega/\epsilon$ as functions of n_0^* for the electron bubble in helium at $T^*=7.7$; DF1 is the result of the density-functional calculation in EP while DF2 is that of the present calculations and IG is from the ideal-gas model found in Ref. 27.

density-functional calculations, respectively. For $n_0^* > 0.10$, our $\Delta\Omega$ is significantly more negative than that found from either of the other theories. This result is consistent with our inclusion of an attractive polarization potential in the interaction which tends to lower the electronic energy in the bubble by lowering the potential energy of the electron in this region of space. As the density becomes smaller, the present $\Delta\Omega$ approaches those found earlier. Also, the density at which the bubble becomes unstable, i.e., $\Delta\Omega=0$, is $n_0^*=0.106$ which is somewhat smaller than in the ideal gas approximation ($n_0^*=0.112$) and in EP ($n_0^*=0.126$). This density is consistent with the observed transition from extended to localized electron states in helium gas.^{8, 27}

In Fig. 3 we compare the density profiles at $n_0^*=0.13$ arising from the three formalisms. Curves IG and DF1 are very similar in that there is a smooth and reasonably broad interface between fluid and the interior of the bubble. The present calculation results in a sharper bubble boundary, as shown by DF2, with all of the fluid excluded from the center of the bubble. The reason for this is presumably the presence of a large, positive short-range contribution to our electron-atom interaction. Any attempt by the fluid atom to enter into the bubble must raise the potential seen by the electron in this region. Consequently, the electron will attempt to expel the fluid atoms even while keeping them close enough that the most attractive part of the electron-atom potential can reach into the bubble. This balance between the negative and positive parts of the electron-atom potential undoubtedly results in the rather abrupt predicted bubble-fluid interface.

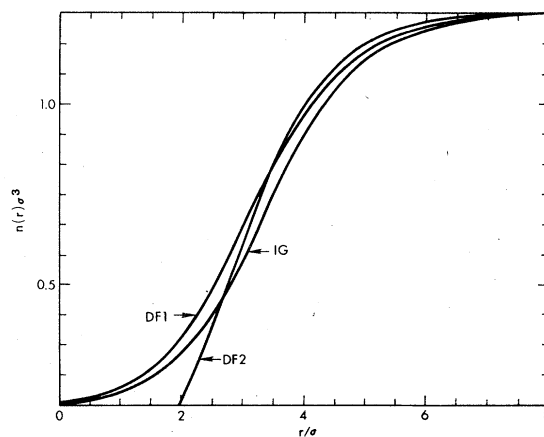


FIG. 3. Reduced density profiles as functions of r/σ for the electron bubble in helium at $T^*=7.7$ and $n_0^*=0.13$; DF1 is from EP, DF2 is the present result, and IG is from the ideal-gas model of Ref. 27.

Of the other rare-gas fluids, only neon is similar to helium in that the localized electron states, if any, are bubbles rather than droplets. In EP, bubble states were found to be stable in liquid Ne in the sense that $\Delta\Omega < 0$ for T^* less than about 1.5 at certain densities n_0^* . Also, these states were predicted to become metastable if the density is either decreased or increased. For temperatures less than the liquid-gas critical temperature, a decrease of n_0^* will eventually lead to a regime where the liquid is metastable against formation of the gas phase. The radius of the bubble grows indefinitely and $\Delta\Omega$ approaches negative infinity. An increase of n_0^* beyond the region of stable bubbles, on the other hand, was found in EP to produce $\Delta\Omega > 0$ and, at some point, a collapse of the bubble.

In Fig. 4 we show our $\Delta\Omega$ in units of ϵ vs n_0^* at selected reduced temperatures between 0.7 and 1.6; behavior similar to that described in EP results at low density according to our calculations, but at high density we predict that the bubble becomes increasingly stable right up to the solidification density. We believe that the difference between the two predictions arises from the inclusion of the attractive polarization potential which, at high fluid density especially, makes the potential well seen by the electron inside of the bubble considerably lower than the one which results from use of a contact potential. We find that at high n_0^* the fluid is completely expelled from the bubble and a sharp interface appears. In Fig. 5 we show the profiles as functions of r/σ at $T^* = 1.5$ for several fluid densities.

The bubble radius R is defined, as in EP, by

$$\frac{4}{3}\pi R^3 = \int d^3r [1 - n(r)/n_0]. \quad (12)$$

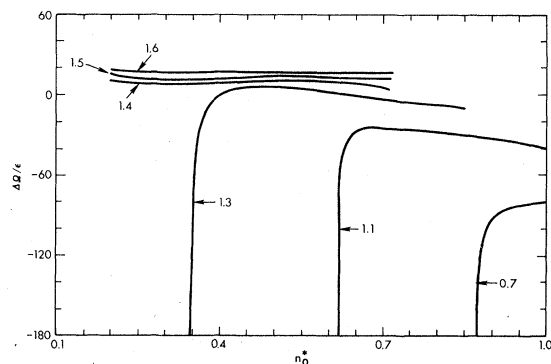


FIG. 4. Reduced free-energy differences $\Delta\Omega/\epsilon$ as functions of n_0^* for electron bubbles in liquid neon at reduced temperatures between 0.7 and 1.6. Each curve is labeled with the value of T^* .

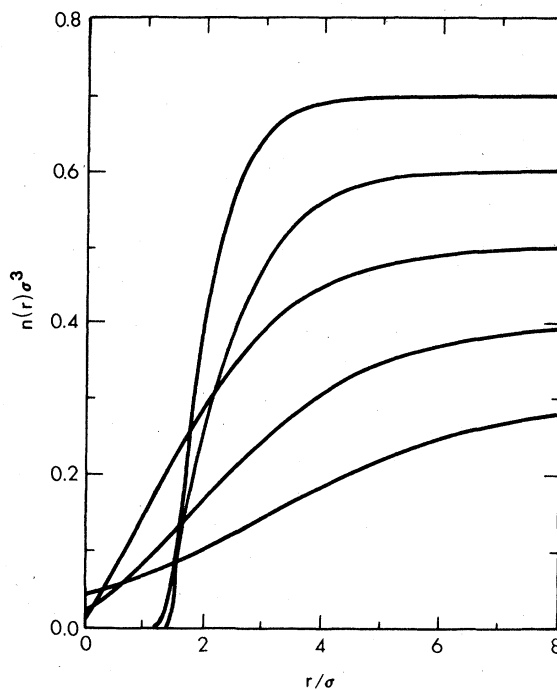


FIG. 5. Reduced density profiles of electron bubbles in neon as functions of r/σ at $T^* = 1.5$. Each curve is labeled with the value of n_0^* .

In Fig. 6 we show R in units of σ vs n_0^* for reduced temperatures from 0.7 to 1.6; the radii are in general about 0.5σ smaller than those given in EP at the same temperatures and densities.

For the heavier rare-gas fluids argon, krypton, and xenon, all theories predict that no bubblelike states exist; extant experimental results support this prediction. Our own search also did not yield any metastable or stable bubbles. It has been proposed,¹³ however, that dropletlike localized

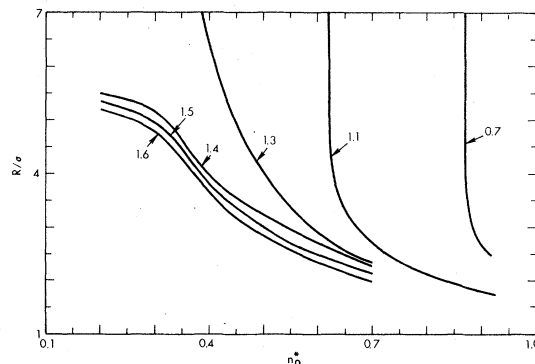


FIG. 6. Bubble radii R in units of σ as functions of n_0^* in neon for a variety of reduced temperatures between 0.7 and 1.6. Each curve is labeled with the value of T^* .

states may exist in these materials, if only briefly, in the gas phase at n_0^* and T^* not far from the critical point. The calculations in EP failed to result in the prediction of any such states. On the other hand, as Freeman and Huang¹⁴ have pointed out, if an appropriate density dependence is introduced into the electron-atom contact potential used in EP, then droplet states will occur.

In order to examine this question further, we have performed additional calculations for argon and xenon using the electron-atom potentials developed in Sec. IIIA. For Ar gas at $T^* = 1.2$, and very close to the gas-liquid phase boundary, we find no localized states; at $T^* = 1.3$, however, we find metastable droplets for n_0^* between 0.10 and the phase boundary ($n_0^* = 0.175$). The relative free energy $\Delta\Omega$ in units of ϵ is 1.9 at $n_0^* = 0.15$. Defining the number of excess fluid particles taking part in this state by

$$N \equiv \int d^3r [n(r) - n_0], \quad (13)$$

we find that $N \cong 45$, independent of the density n_0 .

For Xe gas at $T^* = 1.2$ we find metastable droplets at $n_0^* \geq 0.05$; these droplets have $N \cong 15$. At $T^* = 1.3$, on the other hand, we find droplets with $\Delta\Omega < 0$; specifically, $\Delta\Omega/\epsilon = -5.1$ at $n_0^* = 0.10$ and $\Delta\Omega/\epsilon = -13.3$ at $n_0^* = 0.15$. In the former case $N \cong 80$ and in the latter one $N \cong 100$. Because the localized states are only slightly lower in free energy than the extended states, fluctuations in the energy and particle number of the droplets can easily prevent them from being long lived. We have estimated the fluctuations in a region the size of a droplet at $T^* = 1.3$ and $n_0^* = 0.15$ by regarding it as a system in equilibrium with a reservoir (the uniform fluid) at fixed μ and T . The system occupies a sphere whose radius is essentially that of the droplet 3.5σ . To estimate fluctuations in the number of particles N and energy E we use the standard relations for the grand canonical ensemble,

$$\frac{\langle (\Delta N)^2 \rangle}{N^2} = \frac{kT}{V} \kappa_T \quad (14)$$

and

$$\langle (\Delta E)^2 \rangle = kT^2 C_V + \langle (\Delta N)^2 \rangle \left[\left(\frac{\partial U}{\partial N} \right)_{T,V} \right]^2, \quad (15)$$

where κ_T is the isothermal compressibility of the system, C_V is the heat capacity at constant volume, and U is the internal energy. For the energy we have used the virial expression,

$$U = \frac{3}{2} NkT + \frac{N^2}{2V} \int d^3r g(r) V(r), \quad (16)$$

while the compressibility is obtained from the compressibility equation of state

$$\left(\frac{\partial P}{\partial n} \right)_T = kT [1 - nC(0)], \quad (17)$$

where $C(0)$ is the zeroth Fourier component of the direct correlation function. The correlation functions are obtained from the Percus-Yevick approximation. The root-mean-square (RMS) fluctuation in N is found to be approximately 20 while the RMS fluctuation in the energy is about 75 ϵ . Clearly, droplets of the sort found above will be easily disturbed by fluctuations.

Our predictions for droplet states thus coincide with the observations of Freeman and Huang¹⁴ who find that "of the order of a hundred molecules are involved in a quasidroplet that localized an electron," and "the extent of the electron quasilocalization in dense argon gas near the critical region is less than in xenon at the same relative density and temperature."

IV. SUMMARY

We have applied the approximate density-functional formalism of Ebner, Saam, and Stroud²⁹ to the problem of an excess electron in classical rare-gas fluids. The formalism differs from that used by Ebner and Punyanitya²⁸ in that a model potential consisting of an attractive polarization interaction and a short-range repulsive core has been used to represent the electron-atom interaction. The parameters of the potential are determined from considerations involving low-energy electron-atom *s*-wave scattering phase shifts, screening of the polarization interaction by the other atoms in the fluid, and measured ionization potentials of an excess electron in the various fluids.

The electron bubble and droplet models were used for localized electron states by employing an appropriate trial function with variational parameters to describe the fluid density in the vicinity of the localized electron.

In helium gas we find that the bubble state is significantly more stable than was found in EP at $T^* = 7.7$; also, the boundary of the bubble is predicted to be sharper than in EP. These differences in the predictions are entirely the consequence of the difference between the electron-atom potentials used in the two calculations.

In neon we predict stable bubble states in the liquid near the gas-liquid coexistence curve. These predictions agree with those in EP. However, at higher densities in the liquid phase we find that the bubble states should remain stable in contrast to the prediction of EP that the bubbles will collapse in this region. Further, we find

here that at the higher densities the fluid is totally expelled from the bubble and a sharp interface is formed. Once again, these results must be the consequence of the inclusion in the electron-atom interaction of both long-range attraction and short-range repulsion.

Our results have been obtained using a simple monotonic trial function for the density profile. It is quite possible that a more flexible trial function which can describe nonmonotonic profiles might produce still lower free energies of the bubble states at large n_0 where the interface is very narrow. Even if this is the case, that would not effect our qualitative conclusion that the bubble states are stable in liquid neon in this density regime.

The investigation of EP predicted no dropletlike localized electron state will occur in any of the rare gases. With our physically more reasonable

electron-atom potential, we find metastable droplets in Ar, and metastable or barely stable ones in xenon, in the gas phase close to the critical point. At $T^* = 1.3$ the number of particles involved in the Ar droplets is around 50 and the number in the Xe droplets is about 80 at $n_0^* = 0.10$ and 100 at $n_0^* = 0.15$. The thermal fluctuations in the energy of the droplets are considerably larger in magnitude than the free energy difference between the droplet and uniform gas extended states. Hence the droplets may be expected to be short lived, leading to the electrons being not truly localized but only "quasilocalized." These results are fully consistent with recent observations by Freeman and Huang.^{13, 14}

ACKNOWLEDGMENTS

This work was partially supported by a grant from the National Science Foundation.

- ¹A good review of the work done prior to 1975 is contained in H. T. Davis and R. G. Brown, *Adv. Chem. Phys.* **31**, 329 (1975).
- ²R. L. Williams, *Can. J. Phys.* **35**, 134 (1957).
- ³L. Meyer and F. Reif, *Phys. Rev.* **110**, 279 (1958); **123**, 727 (1961).
- ⁴L. Meyer, S. A. Rice, and R. J. Donnelly, *Phys. Rev.* **126**, 1927 (1962).
- ⁵P. E. Parks and R. J. Donnelly, *Phys. Rev. Lett.* **16**, 45 (1966).
- ⁶J. L. Levine and J. M. Sanders, Jr., *Phys. Rev. Lett.* **8**, 159 (1962).
- ⁷J. L. Levine and J. M. Sanders, Jr., *Phys. Rev.* **154**, 138 (1967).
- ⁸H. R. Harrison and B. E. Springett, *Phys. Lett.* **A35**, 73 (1971).
- ⁹H. R. Harrison, L. M. Sander, and B. E. Springett, *J. Phys. B* **6**, 908 (1973).
- ¹⁰J. A. Jahnke, M. Silver, and J. P. Hernandez, *Phys. Rev. B* **12**, 3420 (1975).
- ¹¹L. Bruschi, G. Mazzi, and M. Santini, *Phys. Rev. Lett.* **28**, 1504 (1972).
- ¹²R. J. Loveland, P. G. LeComber, and W. E. Spear, *Phys. Lett. A* **39**, 225 (1972).
- ¹³S. S.-S. Huang and G. R. Freeman, *J. Chem. Phys.* **68**, 1355 (1978).
- ¹⁴G. R. Freeman and S. S.-S. Huang, *Phys. Rev. A* **20**, 2619 (1979).
- ¹⁵K. Hiroike, N. R. Kestner, S. A. Rice, and J. Jortner, *J. Chem. Phys.* **43**, 2625 (1965).
- ¹⁶T. P. Eggarter, *Phys. Rev. A* **5**, 2496 (1972).
- ¹⁷R. A. Ferrell, *Phys. Rev.* **108**, 167 (1957).
- ¹⁸J. Lekner and A. R. Bishop, *Philos. Mag.* **27**, 297 (1973).
- ¹⁹B. E. Springett, J. Jortner, and M. H. Cohen, *J. Chem. Phys.* **48**, 2720 (1968).
- ²⁰T. Miyakawa and D. L. Dexter, *Phys. Rev.* **184**, 166 (1969).
- ²¹D. W. Swan, *Proc. Phys. Soc. London* **83**, 659 (1964).
- ²²H. Schnyders, S. A. Rice, and L. Meyer, *Phys. Rev. Lett.* **15**, 187 (1965).
- ²³B. Halpern, J. Lekner, S. A. Rice, and R. Gomer, *Phys. Rev.* **156**, 351 (1967).
- ²⁴A. G. Khrapak and I. T. Yakubov, *Zh. Eksp. Theor. Fiz.* **69**, 4042 (1975) [*Sov. Phys.—JETP* **42**, 1036 (1976)].
- ²⁵B. E. Springett, M. H. Cohen, and J. Jortner, *Phys. Rev.* **159**, 183 (1967).
- ²⁶E. Wigner and F. Seitz, *Phys. Rev.* **43**, 804 (1933).
- ²⁷J. P. Hernandez, *Phys. Rev. A* **7**, 1755 (1973); *Phys. Rev. B* **11**, 1289 (1975).
- ²⁸C. Ebner and C. Punyanitya, *Phys. Rev. A* **19**, 856 (1979).
- ²⁹C. Ebner, W. F. Saam, and D. Stroud, *Phys. Rev. A* **14**, 2264 (1976).
- ³⁰J. O. Hirschfelder, C. F. Curtiss, and R. B. Bird, *Molecular Theory of Gases and Liquids* (Wiley, New York, 1954), p. 1110.
- ³¹W. F. Saam and C. Ebner, *Phys. Rev. A* **15**, 2566 (1977).
- ³²C. Ebner, M. A. Lee, and W. F. Saam, *Phys. Rev. A* **21**, 959 (1980).
- ³³T. F. O'Malley, *Phys. Rev.* **130**, 1020 (1963).
- ³⁴P. F. Naccache and M. R. C. McDowell, *J. Phys. B* **7**, 2203 (1974).
- ³⁵D. G. Thompson, *J. Phys. B* **4**, 468 (1971).
- ³⁶T. Heindorff, J. Hoff, and P. Dabkiewicz, *J. Phys. B* **9**, 89 (1976).
- ³⁷C. Ramsauer and R. Kollath, *Ann. Phys. (N.Y.)* **12**, 529 (1932).
- ³⁸See, e.g., L. I. Schiff, *Quantum Mechanics*, 3rd ed. (McGraw-Hill, New York, 1968), Sec. 19.
- ³⁹L. Fox and E. T. Goodwin, *Proc. Cambridge Philos. Soc.* **45**, 373 (1949).
- ⁴⁰W. T. Sommer, *Phys. Rev. Lett.* **12**, 271 (1964).
- ⁴¹W. Tauchert, H. Jungblut, and W. F. Schmidt, *Can. J. Chem.* **55**, 1860 (1977).
- ⁴²W. F. Saam and C. Ebner, *Phys. Rev. A* **17**, 1768 (1978).